Desalination and Water Treatment
www.deswater.com

doi: 10.5004/dwt.2019.23826

148 (2019) 238–247
April

Analysis of the behavior of almond shells biomass in the biosorption of lead(II) and nickel(II) cations in aqueous solution

Salwa Ayed[a], Ali Ghorbel[a], Antonio Comite[b], Taoufik Boubaker[a,*]

[a]*Laboratoire C.H.P.N.R, Faculté des Sciences, Université de Monastir, Avenue de l'Environnement, 5019 Monastir-Tunisie, email: ayed_salwa@yahoo.fr (S. Ayed), ghorbelalifr@yahoo.fr (A. Ghorbel), Tel. 00 216 98652121, email: boubaker_taoufik@yahoo.fr (T. Boubaker)*

[b]*Dipartimento di Chimica e Chimica Industriale, Università degli Studi di Genova, Via Dodecaneso 31, 16146 Genoa, Italy, email: antonio.comite@unige.it (A. Comité)*

Received 14 May 2018; Accepted 21 January 2019

ABSTRACT

Biosorption of lead and nickel onto almond shells from aqueous solution at various temperatures have been investigated kinetically and thermodynamically. The biomass was characterized by SEM and EDX analysis which additionally authenticated the sorption phenomenon. Thermodynamic parameters clearly demonstrated that all the biomass-metal interactions are favourable and exothermic in nature. The experimental data obtained from batch studies revealed that the biosorption kinetics on the biomass may be well described by the pseudo second-order kinetic model. The C_e/q_e values correlated linearly with the equilibrium metal cation concentration in the solution (C_e) according to the Langmuir model, allowing us to determine the biosorption capacity of the biosorbent. About 89.28 and 75.76 mg g^{-1} of Pb(II) and Ni(II) cations, respectively, have been found. The Dubinin–Radushkevich approach is also discussed and showed that the mean free energy (E) obtained for both metal cations suggests a chemical ion-exchange mechanism.

Keywords: Lead and nickel biosorption; Almond shells; Kinetics; Thermodynamics; Ion-exchange mechanism; Isotherm models

1. Introduction

Lead (Pb) and nickel (Ni) are frequently present in water coming from industries waste, causes risks to the aquatic system and consequently human health [1,2]. Lead for instance, which is a pervasive contaminant and extremely toxic in relatively low dosages, is one of the most responsible heavy metals for causing neurological and renal disturbances as well as impairment of cardiovascular system [3]. The current EPA and WHO drinking water standard for lead are 0.05 mg L^{-1} and 10 µg L^{-1}, respectively [4].

Moreover, the excessive intake of nickel by man leads to severe mucosal irritation, widespread capillary damage, hepatic and renal damage, gastrointestinal discomfort and lung cancer [5,6]. The nickel standard for drinking water, according to US-EPA report, is 0.2 mg L^{-1} [6]. In view of the toxicity and to meet regulatory standards for safe discharge, it is necessary to remove lead and nickel from wastewaters/effluents before they are released into the environment.

Various methods have been carried out for the removal of Pb(II) and Ni(II) from industrial wastewater, such as ion exchange, chemical precipitation, coagulation, electrolysis, reverse osmosis processes, electroflotation, ... [7–9]. However, most of these techniques have some disadvantages such as complicated treatment process, high cost, and energy use. Especially in low developing countries, the search for cost effective, competitive and easy to operate methods is strongly recommended. Adsorption is a much more preferable technique for removing heavy metals from polluted waters compared to others because of the ease of operation and cost-effective process [7].

Due to its abundant availability and non-toxicity, several biomaterials are potentially an alternative sorbent for

---

*Corresponding author.

1944-3994 / 1944-3986

metals removal from polluted waters [10–15]. For example, Lansium domesticum peel (LDP), a waste material generated from the fruit consumption, has been evaluated as a biosorbent for Ni(II) ions removal from aqueous media [10]. In recent papers, Basu and co-workers have reported that cucumber peel also exhibit outstanding capability for the removal of Pb(II) from industrial effluent [11].

In our laboratory, we have recently shown that Lignocellulosic sorbent (date pits) could be used as an adsorbent for the removal of Hg(II) and Zn(II) cations from aqueous solutions [12]. This study demonstrates that higher removal activity of the sorbent towards Zn(II) cations. In fact, the maximum biosorption capacities determined by the Langmuir isotherm model were found to be 38.5 mg g^{-1} and 52.6 mg g^{-1} for Hg(II) and Zn(II), respectively.

Continuing the experimental studies on the sorption of heavy metals from polluted waters, the interaction between the almond shells and the Ni(II) and Pb(II) cations is investigated in aqueous solutions to gain further information into the effect biosorption parameters on the reaction mechanism and compare our results with those previously reported for other family of biomaterials.

The objective of this study was to evaluate the potential of almond shells, for the biosorption of lead and nickel from aqueous solutions. In this regard, the effects of pH, contact time and temperature on the biosorption process were examined. Thermodynamic and kinetic parameters are also evaluated. On the other hand, biosorption isotherm models such as Langmuir, Freundlich and Dubinin-Radushkevich were used to analyze the equilibrium biosorption data.

2. Experimental section

2.1. Materials

Almond shells were collected from a local center of shell-removed almond preparation (Sfax-Tunisia). The samples were collected and washed with distilled water to remove the surface-adhered particles and then dried in an oven at 80°C for 3 h until constant weight. The dried biomass was crushed, sieved to obtain particles with an average of 250 µm.

2.2. Analytical analysis

The surface structure and morphology of pristine and metal-loaded biosorbent were characterized using a scanning electron microscope (Zeiss Supra 40 VP, Germany) equipped with an energy dispersive X-ray spectroscopy detector (Zeiss Supra 40 VP, Germany) was used to analyze the variation in chemical elemental composition of biosorbent surface before and after metal biosorption.

All reagents used were of analytical grade (Merck, Germany). Test solutions of binary metal ions were prepared from their chloride salts by serial dilution of stock lead and nickel ion solution (1000 mg L^{-1}) using double deionized water (Milli-Q Millipore 18.2 MΩ cm^{-1} conductivity). The pH of the solution was verified in a 5500 EUTECH pH meter (Thermo Fisher Scientific, USA) using a FET solid electrode calibrated with standard buffer solutions by addition of 0.1 mol L^{-1} HCl and 0.1 mol L^{-1} NaOH solutions as per the required pH value. The metal concentrations were measured using a flame atomic absorption spectrophotometer (Varian Spectraa 55, USA).

2.3. Batch biosorption experiments

Biosorption experiments were carried out using the batch method. In order to optimize the experimental conditions, the batch studies were performed for different metal concentrations (10–350 mg L^{-1}), contact times (10–120 min), pH (2–8) and temperatures (20–50°C). The solutions (50 mL) including the metal ions and 0.5 g of almond shells were shaken during the adsorption experiments in an electrically thermostatic reciprocating shaker (HS 501 digital; IKA Labortechnik) at 150 rpm. At the end of the defined contact time, the contents of the flasks were centrifuged and the liquid was analyzed for metal concentration by using the atomic absorption spectrophotometer.

The percent biosorption and the biosorption capacity at equilibrium (q_e, mg g^{-1}) of metal cation were calculated according to Eqs. (1) and (2) [12], respectively, where C_o (mg L^{-1}) and C_e (mg L^{-1}) are the initial and equilibrium concentrations of metal cation, respectively.

$$Biosorption\ (\%) = \frac{\left(C_o - C_e\right)}{C_o} \times 100 \tag{1}$$

$$q_e = \frac{\left(C_o - C_e\right)}{m} \times 100 \tag{2}$$

3. Results and discussion

3.1. SEM and EDX analysis

As known, the chemistry and the surface morphology of the adsorbent are factors that affect strongly the adsorption process [16]. Scanning electron microscopy (SEM) micrographs and energy dispersive X-ray spectroscopy (EDX) spectra obtained before and after Ni(II) and Pb(II) cations biosorption onto almond shells are presented in Figs. 1 and 2.

These micrographs indicated clearly the deformation and presence of many new shiny bulky particles (in QBSD) over the surface of metal loaded biomass, which were absent on the corrugated surface of the raw almond shells (Fig. 1).

On the other hand, the EDX spectrum of unloaded biomass indicated the presence of K, C, Mg, Si, P, Cl, Na, and O as natural species on the biosorbent (Fig. 2a). These signals are due to X-ray emissions from the polysaccharides and proteins present on the biomass. Whereas, after metal biosorption (Figs. 2b and 2c), elements like potassium, calcium and magnesium signals are almost disappeared indicating that these cations are exchanged with nickel(II) and lead(II) on the surface of the biosorbent.

Consequently, it is reasonable to conclude that Pb(II) and Ni(II) cations can be loaded on the biomaterial surface due to the ion exchange mechanism by K^+, Ca^{2+} and Mg^{2+} cations as shown below:.

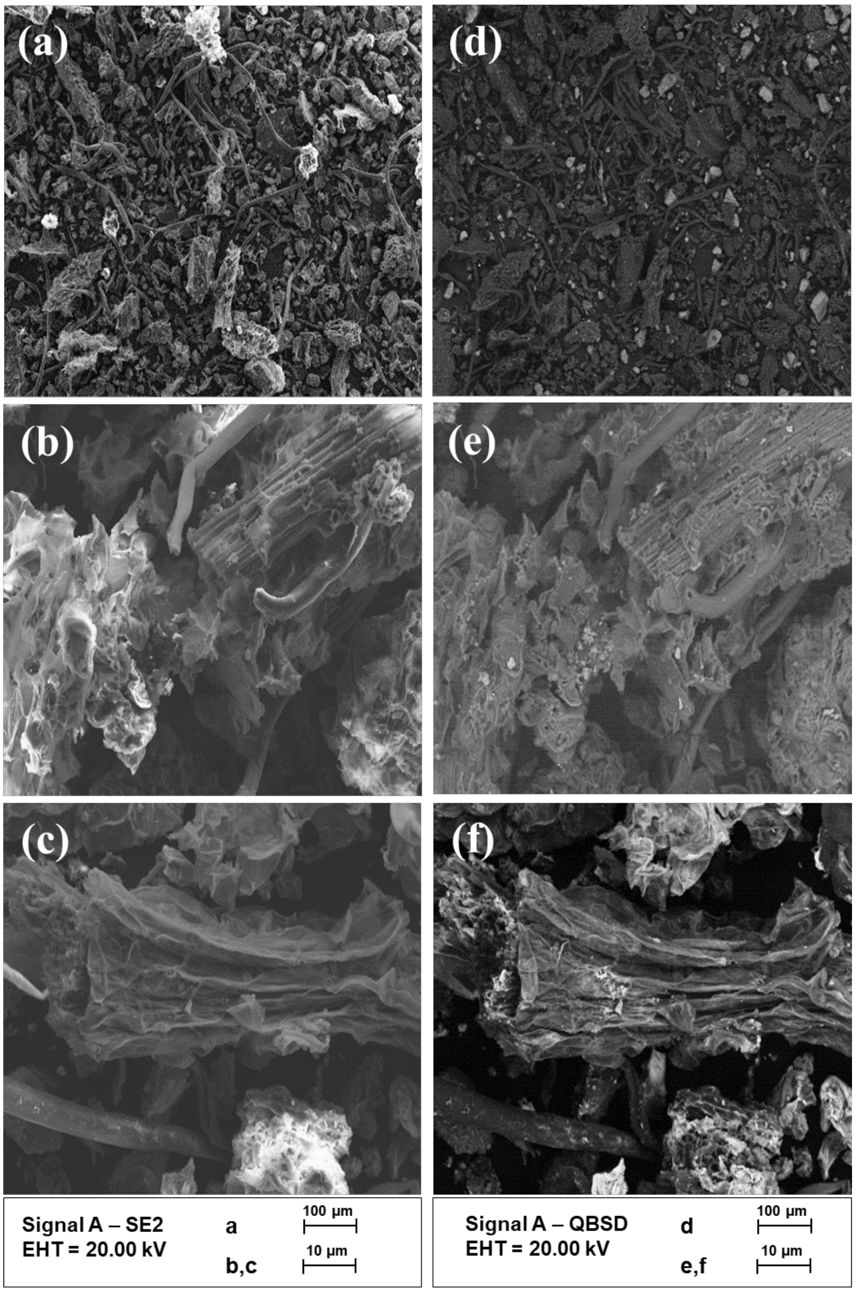

Fig. 1. SEM micrograph of almond shells (a), almond shells + Ni(II) (b) and almond shells + Pb(II) (c) and QBSD of almond shells (d); almond shells + Ni(II) (e) and almond shells + Pb(II) (f).

3.2. Effect of pH solution

Careful examination of literature showed that pH of solution is generally considered as an important parameter in the biosorption process [17,18]. Because the surfaces charge of the biosorbent and the nature of the metal cations in biosorption (ionization degree and speciation) can be affected by the solution pH. In this regard, Fig. 3 describes the % biosorption-pH profiles for the biosorption process of Pb(II) and Ni(II) onto almond shells.

From Fig. 3 we can see that the biosorption efficiency was increased from 18 to 74% for Pb(II) and from 35 to 81% for Ni(II) ions, respectively as pH was increased from 2 to 4. The maximum biosorption was found to be 96% for Pb(II) and 93% for Ni(II) ions at pH 5. Therefore, all the biosorption experiments were carried out at pH 5 in agreement with the results of other authors [19].

At pH 2, the biosorption yields for Pb(II) and Ni(II) are smaller than for any other initial solution pH tested. This result can be attributed to the competition between hydrogen and metal cations on the sorption sites, with an apparent preponderance of hydrogen ions, which restricts the approach of metal ions as in consequence of the repulsive force. By contrast, when the pH increased, the biomass surface was more negatively charged and the functional groups of the biomass were more deprotonated and thus available for metal ions. Above pH equal to 5, insoluble hydroxylated complexes of the metal ions start precipitating from the solution, so that biosorption yields were decreased [20].

3.3. Effect of temperature and contact time

In order to understand the biosorption mechanism of Pb(II) and Ni(II) cations onto almond shells, effects of temperature and contact time [12,21–26] were performed. Fig. 4 displays the biosorption kinetics of these two heavy metal cations in the conditions where the concentration of metal cation is 10 mg L^{-1}, biomass dosage is 10 g L^{-1} and pH = 5.

As shown in Fig. 5, lead (II) and nickel (II) biosorption onto almond shells occurs relatively rapid and equilib-

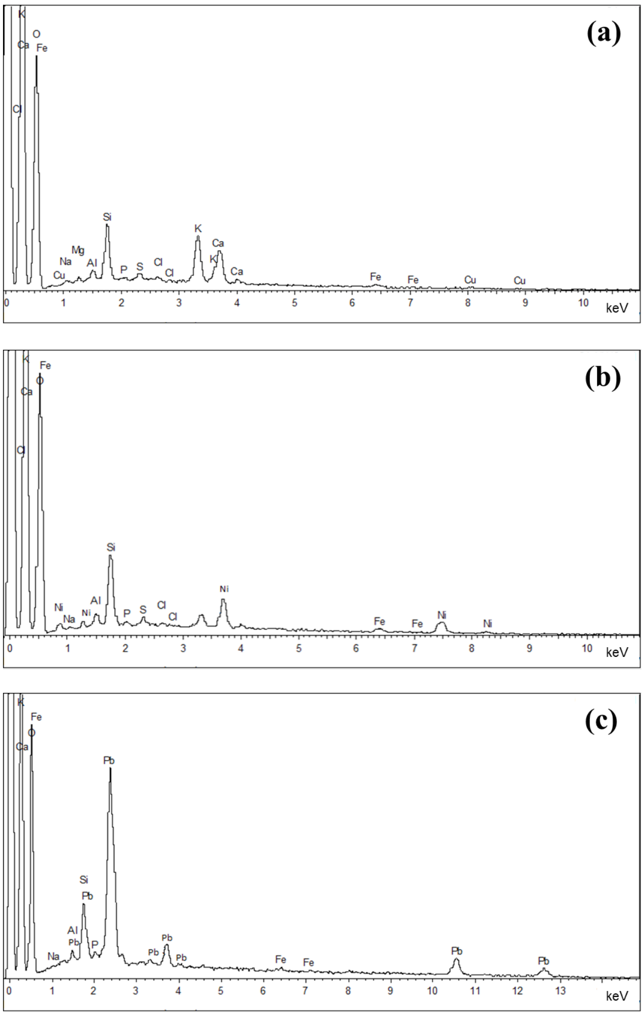

Fig. 2. EDX spectrum of almond shells (a), almond shells + Ni(II) (b) and almond shells + Pb(II).

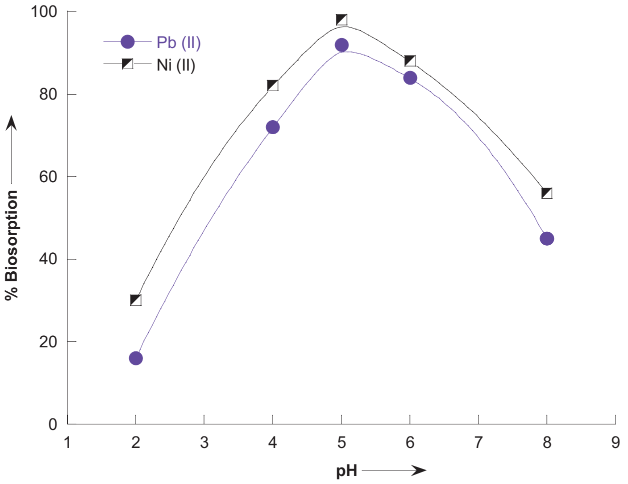

Fig. 3. Effect of pH at 20°C on biosorption of Pb(II) and Ni(II) onto almond shells (metal concentration = 10 mg L^{-1} and biomass dosage = 10 g L^{-1}).

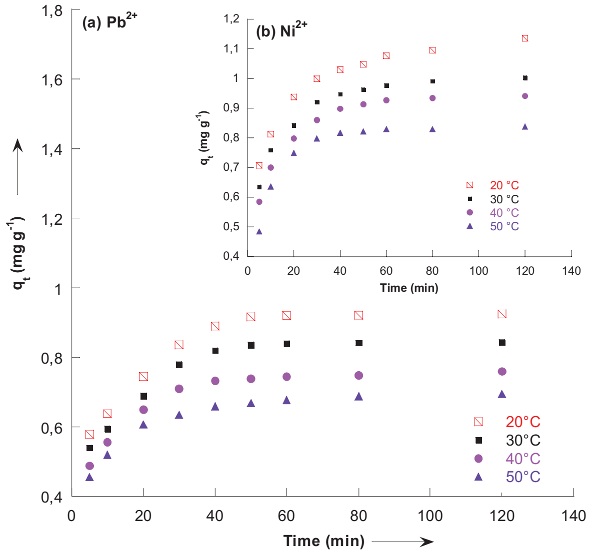

Fig. 4. Effect of contact time and temperature on biosorption of Pb^{2+} (a) and Ni^{2+} (b) onto almond shells with metal concentration = 10 mg L^{-1}, biomass dosage = 10 g L^{-1} and pH = 5.

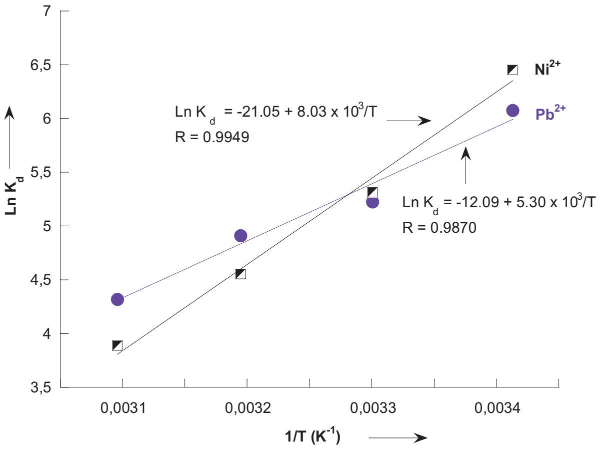

Fig. 5. Determination of thermodynamic parameters for biosorption of Pb(II) and Ni(II) onto almond shells.

rium was reached within 60 min at all temperatures. The rapid biosorption rate that was observed at the beginning of biosorption process may be explained by an increase in the number of active metal binding sites on the biosorbent surface, which would result in an increased concentration gradient between sorbate in the solution and on the biomass surface. After an increase in contact time, the occupation of the remaining vacant sites will be difficult due to the repulsive forces between the Pb(II) and Ni(II) cations on the surface of the adsorbent [27]. The optimum contact time is therefore selected as 60 min for further experiments. On the other hand, the experimental equilibrium biosorption efficiency decreased from 96% to 74% for Pb^{2+} and from 93% to 83% for Ni^{2+} as temperature was raised from 20 to 50°C for the equilibrium time, 60 min. Therefore, the Pb^{2+} and Ni^{2+} biosorption occurred exothermically. The decreasing in biosorption efficiency may be attributed to many parameters such us the relative increase in the escaping tendency of the metal ions from the solid phase to the bulk phase or destructing some active sites on the biosorbent surface [28]. The optimum temperature was selected as 20°C for further biosorption experiments.

3.4. Thermodynamic parameters of biosorption

In order to describe the thermodynamic behaviour of the biosorption of Pb(II) and Ni(II) onto almond shells, thermodynamic parameters, Gibbs free energy change (ΔG^o), standard enthalpy change (ΔH^o) and standard entropy change (ΔS^o) has been analysed using a Van't Hoff Eq. (3) in which K_d represent the distribution coefficient of the adsorbate, R is the universal gas constant (8.314 J mol^{-1} K^{-1}) and T is the absolute temperature (K) [29].

$$Ln\, K_d = \frac{\Delta S^o}{R} - \frac{\Delta H^o}{RT} \tag{3}$$

As can be seen in Fig. 5, excellent straight lines were obtained when the Ln K_d values were plotted *vs.* the reciprocal of the absolute temperature (1/T). The slopes and intercepts of these plots gave the thermodynamic parameters (ΔH^o, ΔS^o, and ΔG^o) which are listed in Table 1.

Analysis of the data in Table 1 reveals that in each reaction series the entropy change (ΔS^o) values is negative, as expected for bimolecular interactions and confirm a decrease in the randomness at the solid-solution interface during the biosorption process [30].

The negative values of ΔH^o indicated that the biosorption process is exothermic in nature involving weak forces of attraction at solid-solution interface [31]. On the other hand, the ΔH° values found in this study for the biosorption of lead (ΔH° = –44.04 kJ mol^{-1}) and nickel (ΔH° = –66.73 kJ mol^{-1}) onto almond shells from aqueous solution, suggesting the implication of chemical biosorption.

Interestingly, ΔH° values of the same order of magnitude have also been reported for the removal of Pb(II) cations from aqueous solutions (ΔH° = –68.07 kJ mol^{-1}) using Cyclosorus Interruptus [32] as well as for the removal of Ni(II) cations (ΔH° = –75.94 kJ mol^{-1}) using compost from olive tree waste [33].

From 20 to 50°C, the values of ΔG^o given in Table 1 for Pb^{2+} and Ni^{2+} are negative, indicating the spontaneity of the biosorption process. It is interesting to note that the ΔG^o values becomes regularly less negative when temperature increased from 293 to 323 K, which suggests that biosorption process is less favourable at higher temperature. This result can also be explained by either a decrease in the number of active groups available at the surface of the sorbent or by a decrease in the mobility of metal cations when temperature increases.

Table 1
Thermodynamic parameters for Pb(II) and Ni(II) cations onto almond shells

Metal cation	T (K)	K_d [a] (mol^{-1} L)	ΔH^o [b] (kJ mol^{-1})	ΔS^o [b] (J mol^{-1} k^{-1})	ΔG^o [c] (kJ mol^{-1})
Pb^{2+}	293	4.36 × 10^2	–44.04	–100.47	–14.60
	303	1.86 × 10^2			–13.60
	313	1.35 × 10^2			–12.59
	323	7.52 × 10^1			–11.57
Ni^{2+}	293	6.35 × 10^2	–66.73	–174.93	–15.62
	303	2.03 × 10^2			–13.88
	313	9.50 × 10^1			–12.13
	323	4.87 × 10^1			–10.39

[a] K_d values calculated from equation $K_d = q_e/C_e$ [12].
[b] ΔH^o and ΔS^o determined in this work from the slope and intercept of plots of Ln K_d *vs* 1/T.
[c] ΔG^o values calculated through the relationship $\Delta G^o = \Delta H^o - T\,\Delta S^o$ [29].

3.5. Biosorption kinetics study

In order to confirm the bimolecular biosorption between almond shells biomass and Pb(II) or Ni(II), the data obtained from kinetic study have been analyzed in accordance with the pseudo second-order kinetic model proposed by Ho et Mckay [Eq. (4)] [34].

$$\frac{t}{q_t} = \frac{1}{k_2 q_e^2} + \frac{t}{q_e} \tag{4}$$

In Eq. (4), k_2 (g mg^{-1} min^{-1}) represents the second-order rate constant of biosorption, q_t and q_e (mg g^{-1}) are the quantity of adsorbed metal cations at time t and at equilibrium status, respectively.

In accord with Eq. (4), excellent linear plots of t/q_t *vs.* t with correlation coefficients >0.9995 were obtained at each temperature studied (Fig. 6). Table 2 summarizes the values of the second-order rate constants (k_2) and the equilibrium biosorption capacity (q_e), which were readily determined from the slope and intercept of these plots. The results clearly show that the reasonable agreement between the equilibrium biosorption capacity calculated by Eq. (2), $q_{e,cal}$, and the experimentally determined value, $q_{e,exp}$, confirms that the kinetic behaviour of lead and nickel biosorption process on almond shells is a second-order interaction. On the other hand, the kinetics data indicates that the rate-controlling step of Pb(II) or Ni(II) cations biosorption might be chemisorption involving valence forces through electron sharing/exchange between metal and active sites, ion exchange reaction, complexation, coordination and/or chelation [35].

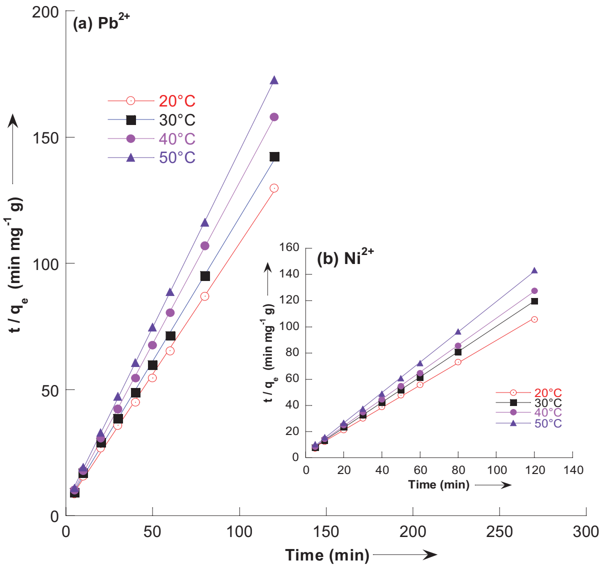

Fig. 6. Pseudo-second-order kinetic plots at different temperatures, pH = 5, biosorbent dosage = 10 g L^{-1} and contact time = 60 min.

Table 2
Pseudo-first-order and pseudo-second-order parameters for the biosorption of Pb(II) and Ni(II) onto almond shells at different temperatures

Cation	T (°C)	k_2 [a] (g mg^{-1} mn^{-1})	$q_{e,exp}$ [a] (mg g^{-1})	$q_{e,cal}$ [b] (mg g^{-1})
Pb^{2+}	20	2.51×10^{-1}	0.97	0.94
	30	3.09×10^{-1}	0.88	0.87
	40	3.82×10^{-1}	0.78	0.83
	50	4.08×10^{-1}	0.72	0.73
Ni^{2+}	20	1.80×10^{-1}	1.17	0.98
	30	2.61×10^{-1}	1.03	0.94
	40	2.82×10^{-1}	0.97	0.88
	50	3.85×10^{-1}	0.86	0.79

[a] k_2 and $q_{e,exp}$ values determined from the slope and intercept of plots of t/q_t *vs* t.
[b] $q_{e,cal}$ values calculated through the relationship $q_e = 100 \times (C_o - C_e)/m$ [12].

On the other hand, analysis of Table 2 reveals that the rate constants k_2, increase regularly with increasing temperature for both metals. This behaviour is interpreted in terms of Arrhenius approach using Eq. (5), where A is the frequency factor, E_a is the activation energy, T is the absolute temperature and R is the universal gas constant [36].

$$Ln k_2 = \frac{-E_a}{RT} + LnA \tag{5}$$

In agreement with relationship (5), satisfactorily straight lines are obtained on plotting the Ln k_2 values *vs.* the reciprocal temperatures (1/T) (Fig. S1 in the Supporting Information). The activation energy (E_a) values associated to the removal of Pb(II) and Ni(II) using almond shells, estimated from these lines over temperatures ranging from 293 to 323 K, were found to be 13.19 and 18.57 kJ mol^{-1}, respectively.

3.6. Langmiur analysis

The data obtained from isotherm experiment have been described by Langmuir model [Eq. (6)], where q_e is the quantity of adsorbed metal cation (mg g^{-1}), C_e is the equilibrium metal cation concentration in the solution (mg L^{-1}), q_{max} is the monolayer biosorption capacity of the biosorbent (mg g^{-1}), and K_L is the Langmuir biosorption constant (L mg^{-1}) relating the free energy of adsorption [37].

$$q_e = \frac{q_{\max} K_L C_e}{1 + K_L C_e} \tag{6}$$

Eq. (6) can be simplified as Eq. (7) under the assumption $K_L C_e < 1$. Accordingly, the plot of q_e values vs C_e is expected to be linear if the above assumption is valid. Whereas at high values of C_e, Eq. (6) simplify to Eq. (8) thus leading to a plateau, from which one can obtained value for q_{max}.

$$q_e = q_{\max} K_L C_e \tag{7}$$

$$q_e = q_{\max} \tag{8}$$

In agreement with Eq. (6), curved plots of q_e *vs.* C_e and approached a plateau at the highest equilibrium metal cation concentration (C_e) were thus observed in Fig. 7, allowing an easy evaluation of values of q_{max} at 20°C : q_{max} = 82.44 mg g^{-1} for Pb(II) and q_{max} = 66.45 mg g^{-1} for Ni(II).

Rewriting Eq. (6) in the form of Eq. (9) allows a new determination of monolayer maximum biosorption capacities q_{max} from the slopes of plots C_e/q_e *vs.* C_e which were linear (Fig. 8). Such linearity confirming monolayer sorption and clearly indicates a saturation of binding sites of the almond shells with negligible interaction among the adsorbed cations. We thus obtain at 20°C q_{max} = 89.28 mg g^{-1} for Pb(II) and q_{max} = 75.76 mg g^{-1} for Ni(II). These values compare well with our earlier determination.

$$\frac{C_e}{q_e} = \frac{1}{q_{\max} K_L} + \frac{C_e}{q_{\max}} \tag{9}$$

In comparison, it is interesting to note that Pb^{2+} showed greater biosorption capacity than Ni^{2+}. This result can be interpreted in terms of covalent index [38], as measured by Eq. (10), where X_m represents the electronegativity of the metal-cation and r is the cationic radius. Thus, inspection of Table 3 reveals that our experimental data agree with the idea that the adsorption capacity increases with the covalent index [39].

$$\text{Covalent index} = X_m^{\,2} \times r \tag{10}$$

In order to confirm the nonexistence of multilayer sorption and heterogeneous distribution of bioorption energies of active sites, Freundlich isotherm model [41] has been considered. The model is described by Eq. (11) where k_f and n are the sorption affinity and the heterogeneity factor, respectively.

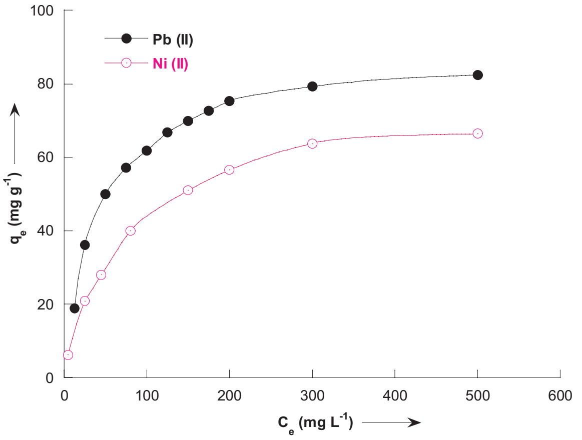

Fig. 7. Biosorption isotherms at 20°C for the removal of Pb(II) and Ni(II) onto almond shells (biomass dosage = 10 g L^{-1}, contact time = 60 min and pH = 5).

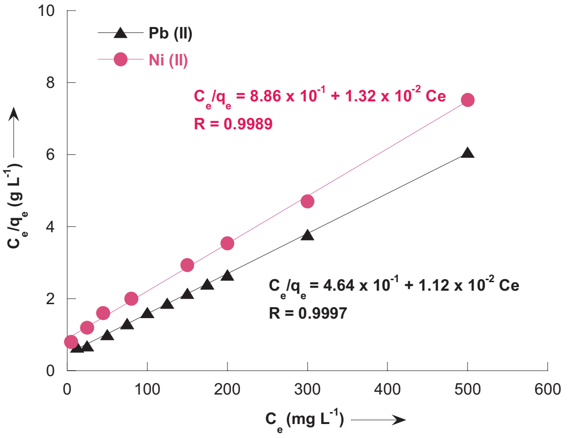

Fig. 8. Langmuir isotherm plots at 20°C for biosorption of Pb(II) and Ni(II) onto almond shells, biomass dosage = 10 g L^{-1}, contact time = 60 min and pH = 5.

Table 3
Covalent index values of Pb^{2+} and Ni^{2+}

Cation	X_m [a]	r [b] (Å)	Covalent index [c]
Pb^{2+}	2.33	1.47	8.0
Ni^{2+}	1.91	1.15	4.2

[a]Ref [40]. [b]Ref [40]. [c]values calculated through the relationship $X_m^2 \times r$ [38].

$$Ln\,q_e = Ln\,k_f + \frac{LnC_e}{n} \tag{11}$$

As can be seen in Fig. 9 unsatisfactory linear correlations were found when Ln q_e were plotted against Ln C_e for both systems studies.

In conclusion, Langmuir isotherms model could be better described the biosorption process than Freundlich model.

In comparing the capacities q_{max} obtained in this work with those previously measured for various biosorbents under similar experimental conditions [42–47] listed in Table 4, it is apparent that our almond shells have higher uptake capacities for both metal cations than most other materials, indicating that almond shells are promising biosorbents for the effective removal of Pb(II) and Ni(II) cations from aqueous solutions.

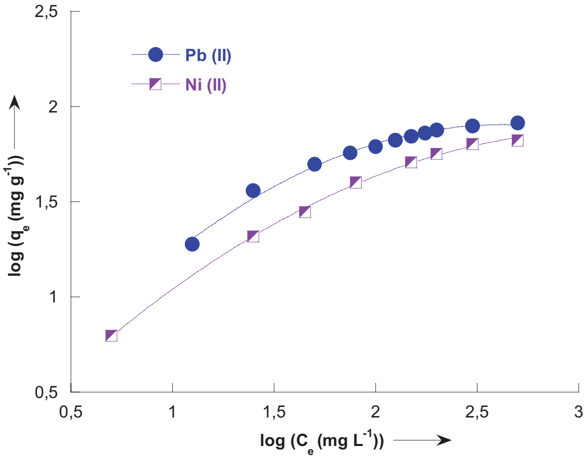

Fig. 9. Freundlich isotherm plots at 20°C for biosorption of Pb(II) and Ni(II) onto almond shells, biomass dosage = 10 g L^{-1}, contact time = 60 min and pH = 5.

Table 4
Comparisons of biosorption potential of various sorbents for lead and nickel removal from aqueous solution

Metal cation	Sorbent	q_{max} (mg g^{-1})	Reference
Pb^{2+}	Peanut shell	38.91	[42]
	Coconut shell	24.24	[43]
	Almond shell (Turkey)	5.43	[44]
	Almond shell (Tunisia)	89.28	Present work
Ni^{2+}	Orange peel	62.89	[45]
	Modified coir pith	38.90	[46]
	Modified sugarcane baggase	54.70	[47]
	Almond shell (Tunisia)	75.76	Present work

3.7. Dubinin-Radushkevich model

In order to analyze the controlling mechanisms involved in solute binding (chemi- versus physic-sorption), the equilibrium data obtained in the present work were also tested with the Dubinin-Radushkevich approach [12]. This linear model can be described by the following relationship

$$\ln q_e = \text{Ln}\, q_m - b\, e \tag{12}$$

where q_e is the amount of metal cations adsorbed on per unit weight of adsorbent (mol g^{-1}), q_m is the maximum adsorption capacity (mol g^{-1}), b is the activity coefficient related to adsorption mean free energy (mol^2 J^{-2}) and e is the Polanyi potential (e = RTLn (1 + 1/C_e)).

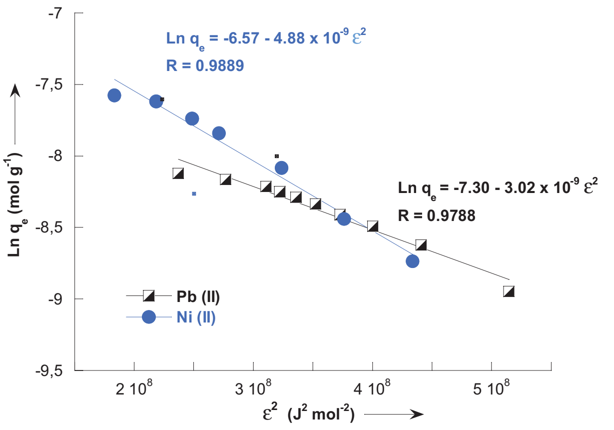

Fig. 10. Dubinin-Radushkevich isotherm plots for biosorption of Pb(II) and Ni(II) onto almond shells at 20°C, biomass dosage = 10 g L^{-1}, contact time = 60 min and pH = 5.

Table 5
Dubinin-Radushkevich parameters for the biosorption of Pb^{2+} and Ni^{2+} onto almond shells

Metal	b (mol^2 J^{-2})	E (kJ mol^{-1})
Pb^{2+}	3.02×10^{-9}	12.85
Ni^{2+}	4.88×10^{-9}	10.12

Plots of Ln q_e *vs.* the ε2 show linear correlations (Fig. 10), from which activity coefficient b according to Eq. (13) were derived (Table 5). It was therefore interesting to use these values of b to estimate the adsorption mean free energy (*E*, kJ mol^{-1}) [Eq. (12)].

$$E = \frac{1}{\sqrt{2\beta}} \tag{13}$$

The mean sorption energies were calculated as 12.85 and 10.12 kJ mol^{-1} for the biosorption of Pb(II) and Ni(II) cations, respectively, (Table 5). This result indicated that the sorption process for the two metal cations onto our almond shells may occurs via chemisorption involving valence forces through sharing or exchange of electrons between biomass and metal [12,48–50].

It has to be noted that similar adsorption mean free energy *E* values have also been reported [51–54], for example, *E* = 11.20 kJ mol^{-1} for lead removal from aqueous media by Moringa Oleifera Bark biosorbent [53] and *E* = 9.81 kJ mol^{-1} for nickel removal from aqueous media by Citrus Limett Peels biosorbent [54].

3.8. Desorption tests

Desorption of Ni(II) and Pb(II) from our biomass was investigated using 0.5 mol L^{-1} HNO_3. As can be seen from Fig. 11, adsorption-desorption was repeated for ten successive cycles with a slight decrease until to 14% in the removal capacity of both metal cations. The obtained results confirmed the ability of the biomass to be regenerated and several times used in the heavy metal uptake process. On the other hand, this result indicates that ion exchange mechanism played a significant role in biosorption of lead and nickel on almond shells.

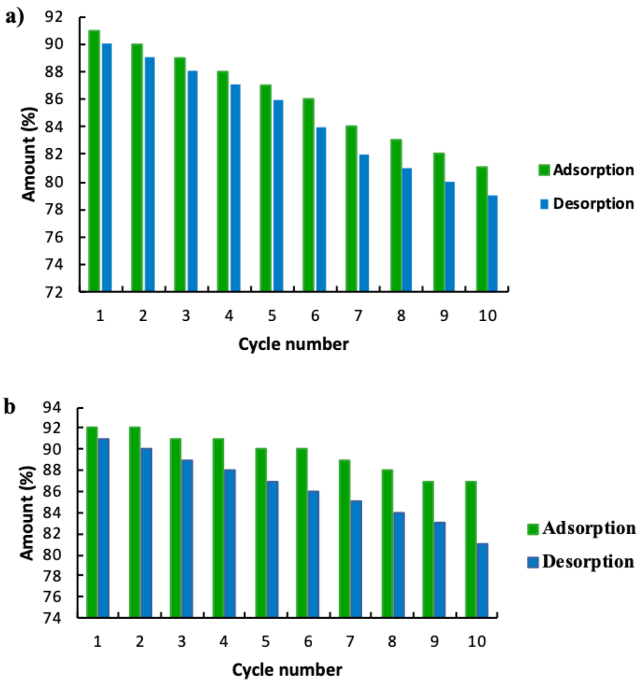

Fig. 11. Desorption tests ((a) Ni^{2+} and (b) Pb^{2+}) at 20°C with initial concentration = 20 mg L^{-1}, contact time = 60 min and 0.5 mol L^{-1} nitric acid as eluent.

4. Conclusion

This study was focused on raw almond shells as a low cost adsorbent for the removal of Pb(II) and Ni(II) cations from aqueous solution. The sorption is affected by various parameters such as contact time, solution pH and temperature. The Langmuir adsorption isotherm model fitted better the experimental data. The monolayer sorption capacity was obtained 89.28 and 75.76 mg g^{-1} for Pb(II) and Ni(II) cations, respectively. The mean free energy values evaluated from the D–R model indicated that the biosorption of both metal ions onto raw almond shells takes place by chemical ion-exchange. The negative ΔH° and negative ΔG° values indicate the exothermic and spontaneous nature of the biosorption process. The overall outcomes indicate that almond shells biomass may be utilized as a promising adsorbent of heavy metal ions and can undoubtedly be competitive with synthesized and low- cost adsorbents.

References

[1] O. Jitar, C. Teodosiu, A. Oros, G. Plavan, M. Nicoara, Bioaccumulation of heavy metals in marine organisms from the Romanian sector of the Black Sea, New Biotechnol., 32 (2015) 369–378.

[2] M. Momčilović, M. Purenović, A. Bojić, A. Zarubica, M. Ranđelović, Removal of lead(II) ions from aqueous solutions by adsorption onto pine cone activated carbon, Desalination, 276 (2011) 53–59.

[3] E.J. Olguín, G. Sánchez-Galván, Heavy metal removal in phytofiltration and phycoremediation: the need to differentiate between bioadsorption and bioaccumulation, New Biotechnol., 30 (2012) 3–8.

[4] V. Gupta, A. Rastogi, Biosorption of lead from aqueous solutions by green algae *Spirogyra* species: Kinetics and equilibrium studies, J. Hazard. Mater., 152 (2008) 407–414.

[5] E. Aranda-García, E. Cristiani-Urbina, Kinetic, equilibrium, and thermodynamic analyses of Ni(II) biosorption from aqueous solution by acorn shell of *Quercus crassipes*, Water Air Soil Pollut., 229 (2018) 119–136.

[6] M.H. Rodiguez, J. Yperman, R. Carleer, J. Maggen, D. Dadi, G. Gryglewicz, B. Van der Bruggen, J.F. Hernández, A.O. Calvis, Adsorption of Ni(II) on spent coffee and coffee husk based activated carbon, J. Environ. Chem. Eng., 6 (2018) 1161–1170.

[7] A. El-Wakil, A.W.M. El-Maaty, F. Awad, Removal of lead from aqueous solution on activated carbon and modified activated carbon prepared from dried water hyacinth plant, J. Anal. Bioanal. Tech., 5 (2014) 1–14.

[8] A. Bhatnagar, A. Minocha, Biosorption optimization of nickel removal from water using *Punica granatum* peel waste, Colloid Surfaces B., 76 (2010) 544–548.

[9] R. Sharma, B. Singh, Removal of Ni(II) ions from aqueous solutions using modified rice straw in a fixed bed column, Bioresource Technol., 146 (2013) 519–524.

[10] Y.F. Lam, L.Y. Lee, S.J. Chua, S.S. Lim, S. Gan, Insights into the equilibrium, kinetic and thermodynamics of nickel removal by environmental friendly *Lansium domesticum* peel biosorbent, Ecotox. Environ. Safe., 127 (2016) 61–70.

[11] M. Basu, A.K. Guha, L. Ray, Adsorption of lead on cucumber peel, J. Clean. Prod., 151 (2017) 603–615.

[12] A. Rezgui, E. Guibal, T. Boubaker, sorption of Hg(II) and Zn(II) ions using Lignocellulosic sorbent (Date Pits), Can. J. Chem. Eng., 95 (2017) 775–782.

[13] S.S. Pillai, B. Deepa, E. Abraham, N. Girija, P. Geetha, L. Jacob, M. Koshy, Biosorption of Cd(II) from aqueous solution using xanthated nano banana cellulose: Equilibrium and kinetic studies, Ecotox. Environ. Safe., 98 (2013) 352–360.

[14] M. Fawzy, M. Nasr, S. Adel, S. Helmi., Regression model, artificial neural network,and cost estimation for biosorption of Ni(II)-ions from aqueous solutions by Potamogeton pectinatus, Int. J. Phytoremediat., 20 (2018) 321–329.

[15] J.G. Flores-Garnica, L. Morales-Barrera, G. Pineda-Camacho, E. Cristiani-Urbina, Biosorption of Ni(II) from aqueous solutions by litchi chinensis seeds, Bioresource Technol., 136 (2013) 635–643.

[16] D. Ozdes, A. Gundogdu, C. Duran, H.B. Senturk, Evaluation of adsorption characteristics of malachite green onto almond shell (Prunus dulcis), Sep. Sci. Technol., 45 (2010) 2076–2085.

[17] A.E. Ofomaja, E.I. Unabonah, N.A. Oladoja, Competitive modeling for the biosorptive removal of copper and lead ions from aqueous solution by Mansonia wood sawdust, Bioresour Technol., 101 (2010) 3844–3852.

[18] I. Alomá, M.A. Martín-Lara, I.L. Rodríguez, G. Blázquez, M. Calero, Removal of nickel (II) ions from aqueous solutions by biosorption on sugarcane bagasse, J. Taiwan Inst. Chem. E., 43 (2012) 275–281.

[19] H. Chen, G. Dai, J. Zhao, A. Zhong, J. Wu, H. Yan, Removal of copper(II) ions by a biosorbent Cinnamomum camphora leaves powder, J. Hazard. Mater., 177 (2010) 228–236.

[20] M.A. Rehab, A.H. Hesham, M.H. Mohamed, F.M. Gihan, Potential of using green adsorbent of heavy metal removal from aqueous solutions: Adsorption kinetics, isotherm, thermodynamic, mechanism and economic analysis, Ecol. Eng., 91 (2016) 317–332.

[21] M. Fawzy, M. Nasr, S. Adel, H. Nagy, S. Helmi, Environmental approach and artificial intelligence for Ni(II) and Cd (II) biosorption from aqueous solution using Typha domingensis biomass, Ecol. Eng., 95 (2016) 743–752.

[22] M. Riaz, R. Nadeem, M.A. Hanif, T.M. Ansari, K. Rehman, Pb(II) biosorption from hazardous aqueous streams using Gossypium hirsutum (Cotton) waste biomass, J. Hazard. Mater., 161 (2009) 88–94.

[23] N. Atar, A. Olgun, Removal of basic and acid dyes from aqueous solutions by a waste containing boron impurity, Desalination, 249 (2009) 109–115.

[24] J.S. Kwon, S.T. Yun, J.H. Lee, S.O. Kim, H.Y. Jo, Removal of divalent heavy metals (Cd, Cu, Pb, and Zn) and arsenic(III) from aqueous solutions using scoria: Kinetics and equilibria of sorption, J. Hazard. Mater., 174 (2010) 307–313.

[25] A. Olgun, N. Atar, Equilibrium, thermodynamic and kinetic studies for the adsorption of lead (II) and nickel (II) onto clay mixture containing boron impurity, J. Ind. Eng. Chem., 18 (2012) 1751–1757.

[26] H. Runtti, S. Tuomikoski, T. Kangas, U. Lassi, T. Kuokkanen, J. Rämö, Chemically activated carbon residue from biomass gasification as a sorbent for iron(II), copper(II) and nickel(II) ions, J. Water Process. Eng., 4 (2014) 12–24.

[27] S.T. Akar, S. Arslan, T. Alp, D. Arslan, T. Akar, Biosorption potential of the waste biomaterial obtained from Cucumis melo for the removal of Pb^{2+} ions from aqueous media: Equilibrium, kinetic, thermodynamic and mechanism analysis, Chem. Eng. J., 185 (2012) 82–90.

[28] A.K. Meena, G.K. Mishra, P.K. Rai, C. Rajagopal, P.N. Nagar, Removal of heavy metal ions from aqueous solutions using carbon aerogel as an adsorbent, J. Hazard. Mater., 122 (2005) 161–170.

[29] S.A. Alavi, H. Zilouei, A. Asadinezhad, Otostegia persica biomass as a new biosorbent for the removal of lead from aqueous solutions, Int. J. Environ. Sci. Technol., 12 (2015) 489–498.

[30] H. Shirzadi, A.N. Ejhieh, An efficient modified zeolite for simultaneous removal of Pb(II) and Hg(II) from aqueous solution, J. Mol. Liq., 230 (2017) 221–229.

[31] C. Hu, P. Zhu, M. Cai, H. Hu, Q. Fu, Comparative adsorption of Pb(II), Cu(II) and Cd(II) on chitosan saturated montmorillonite: Kinetic, thermodynamic and equilibrium studies, Appl. Clay Sci., 143 (2017) 320–326.

[32] K. Zhou, Zhaoguang Yang, Y. Liu, X. Kong, Kinetics and equilibrium studies on biosorption of Pb(II) from aqueous solution by a novel biosorbent: Cyclosorus interruptus, J. Environ. Chem. Eng., 3 (2015) 2219–2228.

[33] I. Anastopoulos, M. Panagiotou, C. Ehaliotis, P.A. Tarantilis, I. Massas, NaOH pretreatment of compost derived from olive tree pruning waste biomass greatly improves biosorbent characteristics for the removal of Pb^{2+} and Ni^{2+} from aqueous solutions, Chem. Ecol., 31 (2015) 724–740.

[34] Y.S. Ho, G. Mckay, D.J. Wase, C. Foster, Study of the sorption of divalent metal ions on to peat, Adsorpt. Sci. Technol., 18 (2000) 639–650.

[35] M. Fawzy, M. Nasr, A. Abdel-Gaber, S. Fadly, Biosorption of Cr (VI) from aqueous solution using agricultural wastes, with artificial intelligence approach. Sep. Sci. Technol., 51 (2016) 416–426.

[36] K.J. Laidler, Chemical Kinetics, Harper & Row Publishers, New-York, 1981.

[37] I. Langmuir, the adsorption of gases on plane surfaces of glass, mica and platinum, J. Am. Chem. Soc., 40 (1918) 1361–1403.

[38] E. Nieboer, W.A.E. McBryde, Free-energy relationships in coordination chemistry. III. A comprehensive index to complex stability, Can. J. Chem., 51 (1973) 2512–2524.

[39] X. Jing, F. Liu, X. Yang, P. Ling, L. Li, C. Long, Adsorption performances and mechanisms of the newly synthesized N, N-di (carboxymethyl) dithiocarbamate chelating resin toward divalent heavy metal ions from aqueous media, J. Hazard. Mater., 167 (2009) 589–596.

[40] C. Can, W. Jianlong, Correlating metal ionic characteristics with biosorption capacity using QSAR model, Chemosphere, 69 (2007) 1610–1616.

[41] H.M.F. Freundlich, Über die adsorption in losungen (adsorption in solution), Z. Physikalische Chemie, 57 (1906) 385–470.

[42] Ş. Taşar, F. Kaya, A. Özer, Biosorption of lead (II) ions from aqueous solution by peanut shells: Equilibrium, thermodynamic and kinetic studies, Chem. Eng. J., 2 (2014) 1018–1026.

[43] I.K.S. Correia, P.F. Santos, C.S. Santana, J.B. Neris, F.H.M. Luzardo, F.G. Velasco, Application of coconut shell, banana peel, spent coffee grounds, eucalyptus bark, piassava (Attalea funifera) and water hyacinth (Eichornia crassipes) in the adsorption of Pb^{2+} and Ni^{2+} ions in water, Chem. Eng. J., 6 (2018) 2319–2334.

[44] Y. Bulut, Z. Tez, Adsorption studies on ground shells of hazelnut and almond, J. Hazard. Mater., 149 (2007) 35–41.

[45] F. Gönen, D.S. Serin, Adsorption study on orange peel: Removal of Ni(II) ions from aqueous solution, Afr. J. Biotechnol., 11 (2012) 1250–1258.

[46] A. Ewecharoen, P. Thiravetyan, W. Nakbanpote, Comparison of nickel adsorption from electroplating rinse water by coir pith and modified coir pith, Chem. Eng. J., 137 (2008) 181–188.

[47] S. Nd. C. Ramos, A.L.P. Xavier, F.S. Teodoro, L.F. Gil, L.V.A. Gurgel, Removal of cobalt(II), copper(II), and nickel(II) ions from aqueous solutions using phthalate-functionalized sugarcane bagasse: Mono- and multicomponent adsorption in batch mode, Ind. Crop. Prod., 79 (2016) 116–130.

[48] B.R. Naik, C. Suresh, N.S. Kumar, K. Seshaiah, A.V.R. Reddy, Biosorption of Pb(II) and Ni(II) ions by chemically modified Eclipta alba stem powder: Kinetics and equilibrium studies, Sep. Sci. Technol., 52 (2017) 1717–1732.

[49] M.R. Huang, H.J. Lu, X.G. Li, Synthesis and strong heavy-metal ion sorption of copolymer microparticles from phenylenediamine and its sulfonate, J. Mater. Chem., 22 (2012) 17685–17699.

[50] Z.B. Bouabidi, M.H. El-Naas, D. Cortes, G. McKay, Steel-making dust as a potential adsorbent for the removal of lead (II) from an aqueous solution, Chem. Eng. J., 334 (2018) 837–844.

[51] M.G. Mahfouz, A.A. Galhoum, N.A. Gomaa, S.S. Abdel-Rehem, A.A. Atia, T. Vincent, E. Guibal, Uranium extraction using magnetic nano-based particles of diethylenetriamine-functionalized chitosan: Equilibrium and kinetic studies, Chem. Eng. J., 262 (2015) 198–209.

[52] F. Rubio, A.C.G. Jr., D.C. Dragunski, C.R.T. Tarley, A.P. Meneghel, D. Schwantes, A Crambe abyssinica seed by-product as biosorbent for lead(II) removal from water, Desal. Water Treat., 53 (2015) 139–148.

[53] A.E. Ofomaja, E.B Naidoo, S.J. Modise, Biosorption of copper(II) and lead(II) onto potassium hydroxide treated pine cone powder, J. Environ. Manage., 91 (2010) 1674–1685.

[54] D.H.K. Reddy, Y. Harinath, K. Seshaiah, A.V.R. Reddy, Biosorption of Pb(II) from aqueous solutions using chemically modified Moringa oleifera tree leaves, Chem. Eng. J., 162 (2010) 626–634.

[55] S. Singh, S.R. Shukla, Theoretical studies on adsorption of Ni(II) from aqueous solution using Citrus limetta peels, Environ. Prog. Sustain., 36 (2017) 864–872.